JPn Neuroscience
The Journal of Physiology

Accurate and representative decoding of the neural drive to muscles in humans with multi-channel intramuscular thin-film electrodes

Silvia Muceli[1], Wigand Poppendieck[2], Francesco Negro[1], Ken Yoshida[3], Klaus P. Hoffmann[2], Jane E. Butler[4], Simon C. Gandevia[4] and Dario Farina[1]

[1]*Department of Neurorehabilitation Engineering, Bernstein Focus Neurotechnology Göttingen, Bernstein Center for Computational Neuroscience, University Medical Center Göttingen, Georg-August University, 37075 Göttingen, Germany*
[2]*Department of Medical Engineering and Neuroprosthetics, Fraunhofer Institute for Biomedical Engineering, 66386 St Ingbert, Germany*
[3]*Biomedical Engineering Department, Indiana University-Purdue University Indianapolis (IUPUI), Indianapolis, IN 46202-5160, USA*
[4]*Neuroscience Research Australia, Barker St, Randwick and University of New South Wales, Sydney, NSW 2031, Australia*

Key points

- Intramuscular electrodes developed over the past 80 years can record the concurrent activity of only a few motor units active during a muscle contraction.
- We designed, produced and tested a novel multi-channel intramuscular wire electrode that allows *in vivo* concurrent recordings of a substantially greater number of motor units than with conventional methods.
- The electrode has been extensively tested in deep and superficial human muscles.
- The performed tests indicate the applicability of the proposed technology in a variety of conditions.
- The electrode represents an important novel technology that opens new avenues in the study of the neural control of muscles in humans.

Abstract We describe the design, fabrication and testing of a novel multi-channel thin-film electrode for detection of the output of motoneurones *in vivo* and in humans, through muscle signals. The structure includes a linear array of 16 detection sites that can sample intramuscular electromyographic activity from the entire muscle cross-section. The structure was tested in two superficial muscles (the abductor digiti minimi (ADM) and the tibialis anterior (TA)) and a deep muscle (the genioglossus (GG)) during contractions at various forces. Moreover, surface electromyogram (EMG) signals were concurrently detected from the TA muscle with a grid of 64 electrodes. Surface and intramuscular signals were decomposed into the constituent motor unit (MU) action potential trains. With the intramuscular electrode, up to 31 MUs were identified from the ADM muscle during an isometric contraction at 15% of the maximal force (MVC) and 50 MUs were identified for a 30% MVC contraction of TA. The new electrode detects different sources from a surface EMG system, as only one MU spike train was found to be common in the decomposition of the intramuscular and surface signals acquired from the TA. The system also allowed access to the GG muscle, which cannot be analysed with surface EMG, with successful identification of MU activity. With respect to classic detection systems, the presented thin-film structure enables recording from large populations of active MUs of deep and superficial muscles and thus can provide a faithful representation of the neural drive sent to a muscle.

DOI: 10.1113/JP270902

(Received 8 May 2015; accepted after revision 13 July 2015; first published online 15 July 2015)
Corresponding author D. Farina: Department of Neurorehabilitation Engineering, Bernstein Focus Neurotechnology Göttingen, Bernstein Center for Computational Neuroscience, University Medical Center Göttingen, Georg-August University, Von Siebold-Str. 6, 37075 Göttingen, Germany. Email: dario.farina@bccn.uni-goettingen.de

Abbreviations ADM, abductor digiti minimi; AP, action potential; CKC, convolution kernel compensation; CoV, coefficient of variation; EMG, electromyogram; GG, genioglossus; ISI, inter-spike interval; MN, motoneurone; MU, motor unit; MVC, maximal voluntary contraction; TA, tibilias anterior.

Introduction

Synaptic input converging on α-motoneurones (MNs) is transformed into output trains of action potentials (APs). Axons from MNs synapse with skeletal muscles at neuromuscular junctions in which APs from the axons of a MN are converted into APs of the innervated muscle fibres. The MN and its innervated muscle fibres constitute the motor unit (MU) (Liddell & Sherrington, 1925). The ensemble of AP trains from the pool of α-MNs innervating a muscle constitutes the neural drive to the muscle.

The muscle provides a convenient interface to access the neural drive. In fact, due to the safety margin of the neuromuscular junction, an axonal AP leads inevitably to an AP of the corresponding MU. Therefore, recordings from muscle fibres reflect the spike trains of the MN axons. Since each α-MN activates an AP in all muscle fibres it innervates, the muscle acts as a biological amplifier of the efferent activity providing signals with high signal-to-noise ratio (Farina & Negro, 2012).

Electromyogram (EMG) can be detected at the skin overlying the muscle (surface EMG) or from the muscle fibres (intramuscular EMG). With surface electrodes, the muscle fibre APs are filtered by the volume conductor between the muscle and the electrodes. Therefore, classic surface EMG recording systems are influenced by electrode position (Mesin *et al.* 2009), amplitude cancellation (Keenan *et al.* 2005) and cross-talk (Farina *et al.* 2002), and provide only a rough estimation of the neural drive. To circumvent these limitations, recent advances in surface EMG decomposition techniques (Holobar & Zazula, 2007) have allowed the extraction of MU activity from multi-channel surface EMG obtained by high-density grids of electrodes. Surface EMG decomposition, however, only allows identification of superficial MUs (Farina *et al.* 2010). Moreover, the number of MUs that can be discriminated from surface EMG signals depends on the number of available channels (Farina & Enoka, 2011), which may be limited in small muscles.

Direct recording of AP trains of MUs is traditionally performed with needles or wire electrodes (Adrian & Bronk, 1929), which are more selective than surface electrodes. Therefore, MUs accessed with a conventional intramuscular electrode represent only a tiny fraction of the population of MUs active during that contraction (Merletti & Farina, 2009).

Multi-wire systems (De Luca & Forrest, 1972) have been used previously to record from slightly different muscle locations. However, there are no indwelling electrodes that provide spatial sampling of intramuscular activity over a large muscle area. Sampling from different portions of a muscle is currently done through serial recordings of MU activity in different muscle sites, e.g. moving a needle electrode inside a muscle or inserting the needle in different positions (e.g. Saboisky *et al.* 2006, 2007) or regional placement of multiple fine wire electrodes within a muscle (e.g. Héroux *et al.* 2014).

We describe a novel intramuscular electrode that allows concurrent sampling of the activity of MUs from a large portion of the muscle cross-section. Polyimide thin-film technology was used, which allows the building of multiple small (and therefore selective) detection sites with reproducible site geometry, on a thin (10–20 μm) and flexible substrate (Stieglitz *et al.* 2000). Thin-film structures have been employed for recording from nerves (Yoshida & Stein, 1999) and muscles in animals (Farina *et al.* 2008); however, the electrode design previously proposed was not suitable for human recordings.

Here we report the development and testing of a thin-film multi-channel electrode for intramuscular recordings in humans. The structure includes 16 small detection sites arranged in a linear configuration. The rationale was to combine selectivity and spatial sampling to obtain an electrode that can sample MU activity from much of the muscle cross-section. The electrode we devised enables recording from large populations of MUs and thus the obtention of a faithful representation of the neural drive to a muscle. The electrode has been tested in several muscles of healthy human subjects during contractions at various forces. Preliminary results have been presented in conference abstracts (Poppendieck *et al.* 2013, 2014*a*).

Methods

Intramuscular thin-film electrode

Figure 1*A* shows a picture of the multi-channel thin-film structure. It contains a linear array of 16 detection sites close to the tip (Fig. 1*B*) and a connection pad array for interfacing with external hardware. The structure is

attached to a 25 G hypodermic needle, used to facilitate its insertion, with a guiding filament. The structure has a total length of 6.81 cm, and is U-shaped, with the two filaments 420 μm and 100 μm wide, and 20 μm thick (Fig. 1*D*). The narrower filament is hooked to a cannula that serves as a guide during the insertion (see Insertion procedure). The wider filament contains 16 oval-shaped platinum active sites (140 μm $\times$ 40 μm, Fig. 1*G*) arranged in a linear configuration (1 mm inter-site spacing) close to the tip (Fig. 1*B* and *F*). The structure was equipped with a 3D printed box that facilitates handling and transportation (Fig. 1*C*).

Manufacturing process

The thin-film electrode structure was built using micro-fabrication processes (Fig. 2). A 4 inch silicon wafer was used as a platform for the electrode production. Eighteen structures were produced in each wafer. A 10 μm thick polyimide layer was deposited on the wafer by spin coating and cured at 350°C. A photoresist was then deposited and structured by photolithography. A 300 nm thick gold metallization layer was sputtered on the polyimide, and 10 μm wide tracks with contact pads were formed by removing the spare metal by a lift-off technique. Another 300 nm thick metallic layer of platinum for the electrode contacts was sputtered on the polyimide and patterned by a lift-off process. Subsequently, a second 10 μm polyimide layer was spin coated and cured, and the electrode contacts and contact pads were opened by reactive ion etching using an aluminium mask. The separated thin-film structures were then removed from the wafer using tweezers. The structures were inspected under the microscope after each step of the manufacturing process to verify that there were no failures in the metallization and only the structures with all electrodes functional (neither open contacts nor short-circuits) were selected (~17/18 on average). The flexible polyimide foil of each structure was attached to a rigid polymer adapter (FR4) using a modified bonding technique (MicroFlex) (Meyer *et al.* 2001). A plug (Harwin M50-4900845 connector) was soldered to the adapter as the interface with external hardware (Fig. 1*E*). The final assembly of the thin-film electrode structure is shown in Fig. 1*A*.

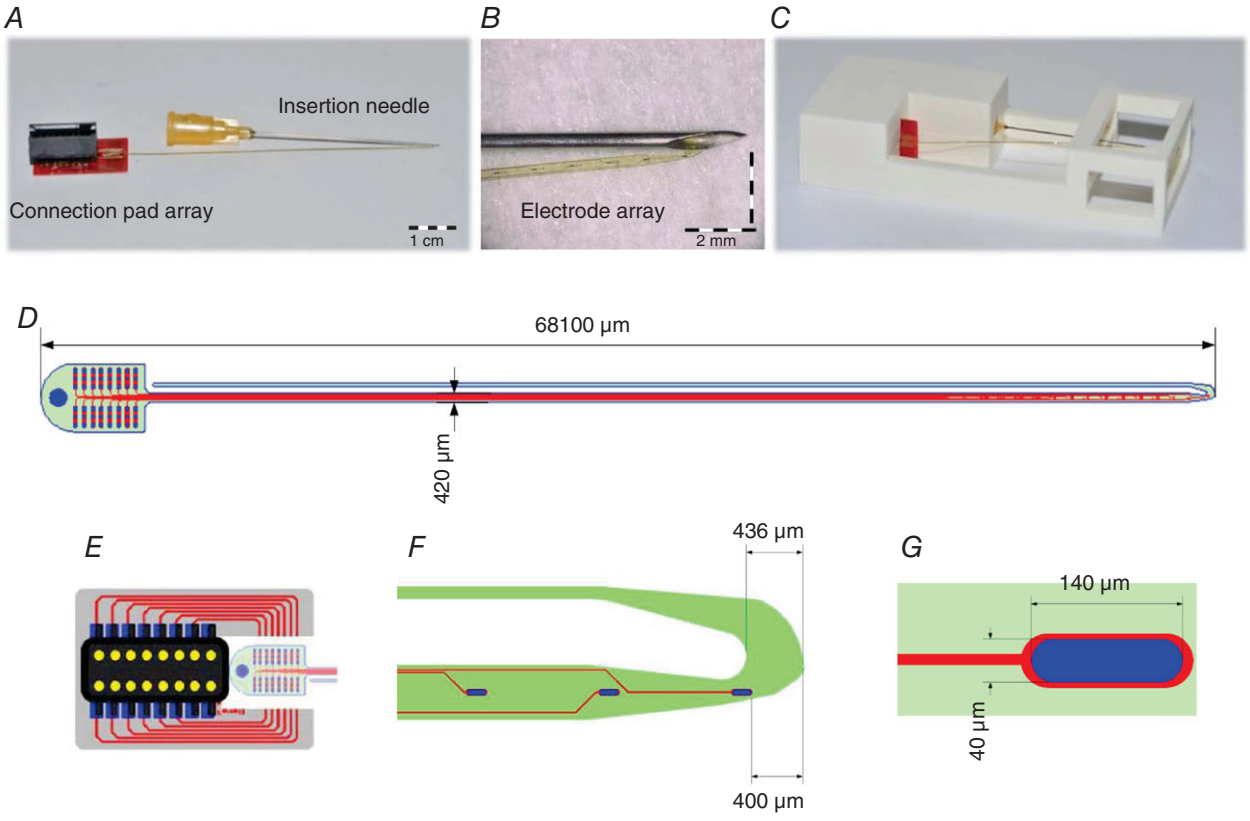

Figure 1. Thin-film electrode
A, the final assembly of the thin-film electrode structure. *B*, a close-up of the structure tip with the 16 detection sites. *C*, box for transportation. *D*, the whole structure. *E*, FR4 adapter and plug where the polyimide foil is attached. *F*, dimension of the tip. *G*, dimension of each oval-shape platinum electrode site at the structure tip.

Impedance

To optimize the electrochemical properties and to reduce interface impedance of the electrodes, the electrode contacts were coated with microrough platinum using electroplating from an aqueous solution of hexachloroplatinic acid (Poppendieck *et al.* 2014*b*). The microrough structure yields an increase in the effective surface area. Electrode impedance spectroscopy was performed in the range 0.1 Hz to 100 kHz. Figure 3 shows the results of the impedance spectroscopy for one of the structures used in the study. It is visible that all 16 contacts have similar impedance. Coating with microrough platinum reduced impedance by about one order of magnitude. At 1 kHz, absolute impedance was ∼100 kΩ for the uncoated electrodes, and ∼10 kΩ for the electrodes coated with microrough platinum. The measurement of impedance served also to confirm the absence of open contacts and/or short-circuits resulting from the manufacturing process.

Insertion procedure

The electrode structure was designed for acute implantation. Classical intramuscular wire electrodes are built passing a strand of coated metal wire through the shaft of a hypodermic needle (Basmajian & Stecko, 1962). Intramuscular signals are detected from the uninsulated part of the wire, bent at the tip of the needle. Different selectivity can be achieved exposing only the wire cross-section or removing part of the coating. The needle is used only as an introducer and removed after the insertion, leaving only the wire inside the muscle.

The same procedure cannot be applied directly to the developed electrode structure, as the adapter with the plug is too wide to fit through the needle when removing it. To circumvent this problem, the structure had a U-shape with a guiding filament (apart from the one containing the electrode contacts) whose only function was to facilitate the insertion of the structure inside the muscle. The guiding filament was threaded into a standard hypodermic

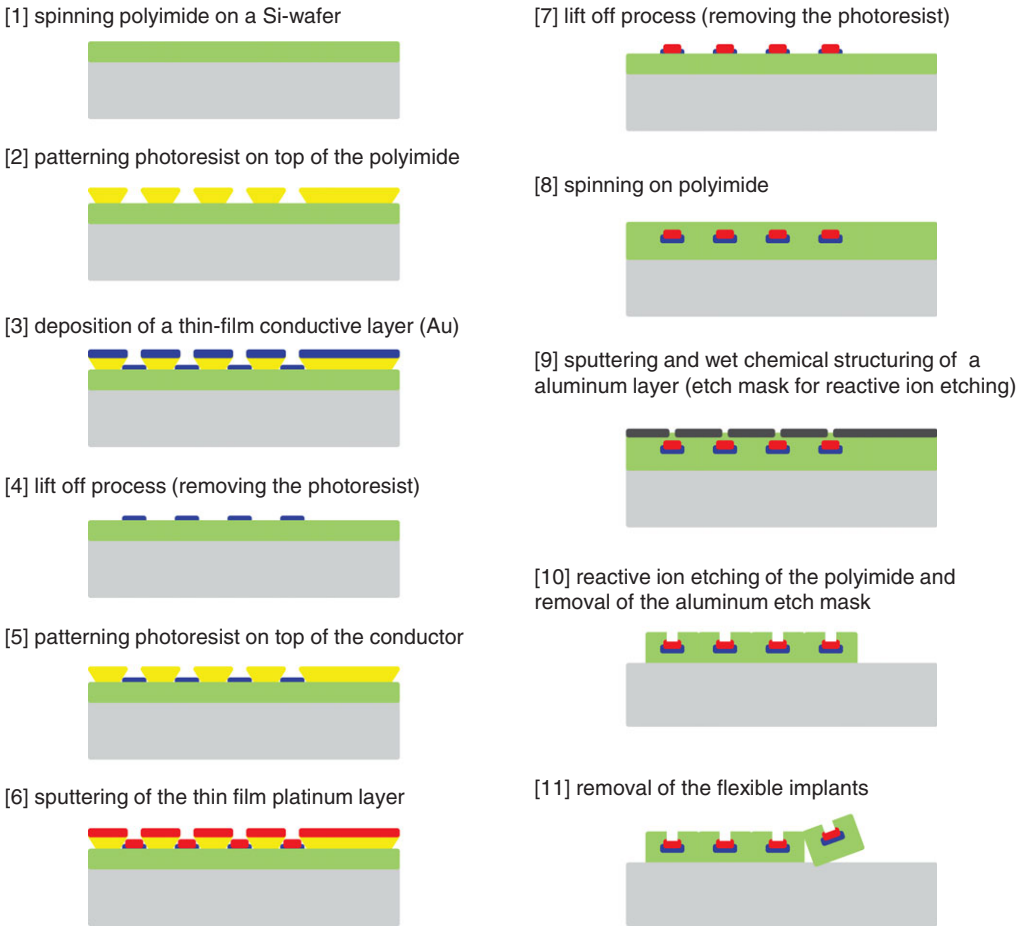

Figure 2. Schematic diagram of the microfabrication process for development of the thin-film electrode structure
Two layers of metal are sandwiched between two layers of polyimide. The polyimide is then opened on the top side to expose the electrode sites.

needle, used to insert the entire structure inside the muscle, and then removed together with the recording portion of the electrode as done for classic intramuscular wire electrodes. The width of the filament with the electrode contacts is determined by the area of each electrode contact and the number of tracks (and thus the number of electrode contacts) running towards the adapter. In the design that we proposed, the wider filament section was 420 μm × 20 μm, which is negligible with respect to the needle section. Therefore, the presence of the filament outside the needle does not cause any pain during the insertion procedure additional to the usual pain resulting from the needle itself. The guiding filament can be even narrower because it does not contain any electronics and thus it can be inserted in a small-gauge needle. In the experiments, we used 25 gauge needles (100 Sterican, B. Braun, Melsungen, Germany).

Preliminary tests on rubber showed that the guiding filament might break during the insertion procedure due to the contact of the polyimide with the sharp edge of the needle bevel. Therefore, the needle bevel was smoothed with a laser (Picco Laser, O.R. Lasertechnologie, Dieburg, Germany) prior to threading the guiding filament inside the needle. With this expedient, the occurrence of breaking was reduced to about 10% of the insertions. It is worth noting that even in case of breaking, the two filaments can be easily withdrawn from the muscle as both filaments exit from the skin. In spite of the low cut resistance to sharp objects, thin-film electrodes built with the same materials and technology as those used in this study are characterized by long-term flexibility and strong resistance to traction forces related to insertion and muscle movement during contractions (Hoffmann & Koch, 2005; Farina *et al.* 2008; Rossini *et al.* 2010).

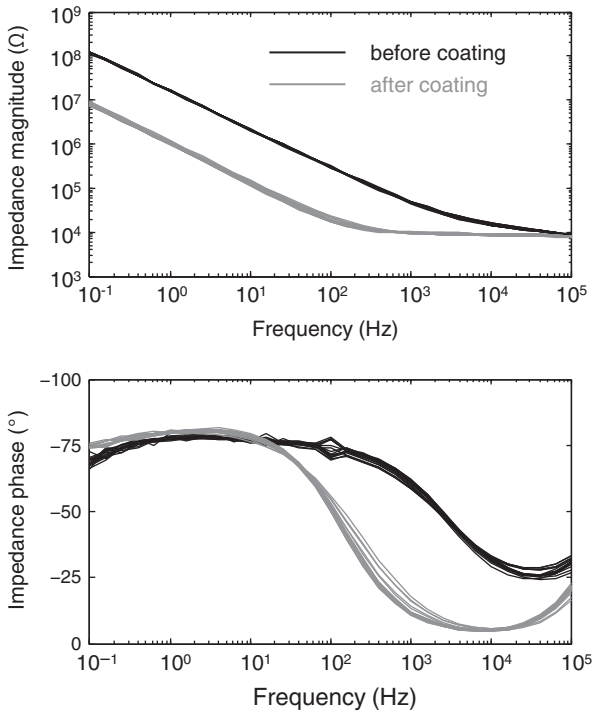

Figure 3. Impedance measurements
Representative example of the impedance of the 16 detection sites before (black) and after (grey) coating with microrough platinum.

Experimental procedure

We present the results of tests in which three muscles were targeted: the abductor digiti minimi (ADM, Experiment 1), the tibialis anterior (TA, Experiment 2), and the genioglossus muscle (GG, Experiment 3). These muscles were chosen because of their different sizes and depths, and because they are commonly analysed using invasive EMG. Three men participated in one experiment each (39, 38 and 35 years old). Experiments were approved by the Ethical Committee of the University Medical Center Göttingen (Experiments 1 and 2) and the Human Research Ethics Committee of the University of New South Wales (Experiment 3) and conducted according to the *Declaration of Helsinki* (2008).

Experiments 1 and 3 aimed at showing that the multi-channel thin-film structure can be used to record from populations of motor units of superficial and deep muscles, respectively. The aim of Experiment 2 was to show that motor unit activity extracted from the proposed intramuscular multi-channel electrode and high-density surface electrodes over a superficial muscle are complementary.

In all experiments, the needle insertion was guided by ultrasound. In Experiments 1 and 2, the hand and foot, respectively, were constrained in an instrumented brace that measures the exerted force (Fig. 4*A* and *B*). The EMG electrodes were placed after determination of the maximal voluntary contraction (MVC). In Experiment 1, the thin-film electrode structure was inserted with an angle of approximately 30 deg with respect to the direction of the muscle fibres. The isometric abduction force of the little finger was measured with a load cell (Interface, Scottsdale, AZ, USA). In Experiment 2, two thin-film structures were inserted into the TA muscle ∼2 cm apart in the longitudinal direction, approximately perpendicularly to the skin. The insertion depths of the proximal and distal electrodes were 3.4 and 4 cm, respectively. Moreover, a high-density grid of 5 × 13 surface EMG electrodes with 8 mm inter-electrode distance (OT Bioelettronica, Turin, Italy) was positioned beside the two thin-film structures, medially. The subject was seated in the chair of a Biodex System 3 (Biodex Medical Systems Inc., Shirley, NY, USA) with the right leg and foot stably fixed. The ankle dorsiflexion force was measured using an ATI Omega 160 force transducer (ATI, Apex, NC, USA) attached to the foot plate. In the first two experiments the thin-film electrodes were left inside

the muscle for about 2 h during which the subject performed some extra voluntary contractions. This was done to evaluate the signal quality over time. In Experiment 3, the subject lay supine and the thin-film electrode structure was inserted 10 mm posterior to the genial tubercle of the mandible and 3 mm from the midline perpendicularly to the skin and 3.8 cm deep. The subject breathed quietly with the mouth closed through a sealed close-fitting nose mask connected via a two-way valve (Hans Rudolph, 1400, Shawnee, KS, USA) to a pneumotachometer (Fig. 4*C*).

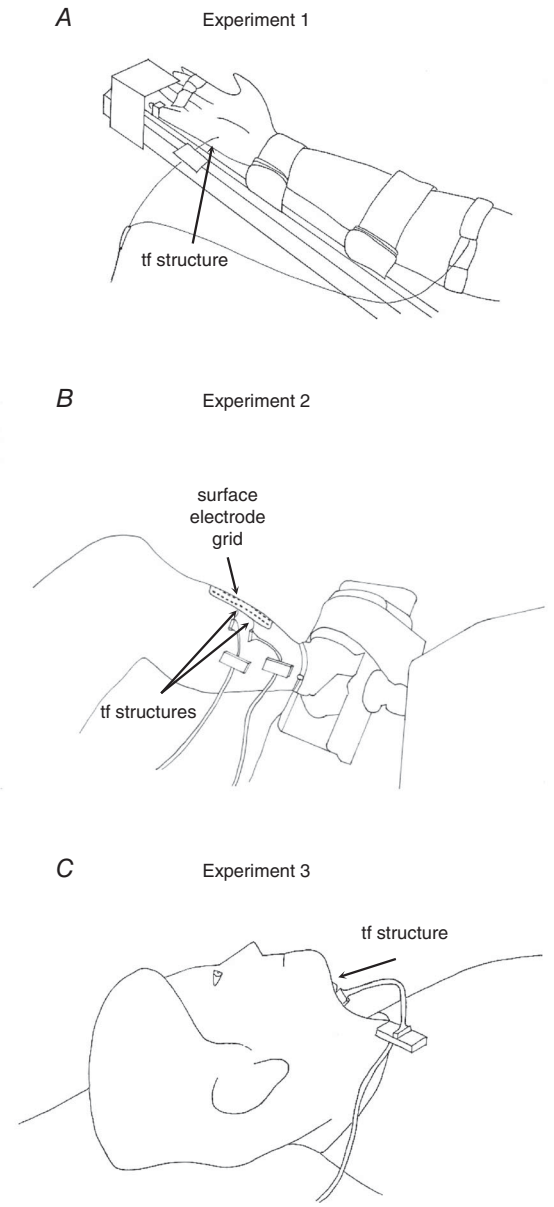

Figure 4. Experimental set-up
A, Experiment 1: the thin-film electrode was inserted in the abductor digiti minimi muscle and the subject was instructed to abduct the little finger at 10 and 15% of the maximal force. *B*, Experiment 2: electromyographic signals were recorded from the tibialis anterior muscle with two intramuscular thin-film structures and a grid of surface electrodes while the subject dorsiflexed the ankle exerting 10, 20 and 30% of the maximal force. *C*, Experiment 3: the subject lay supine and breathed quietly with the thin-film structure inserted into the genioglossus muscle.

Intramuscular EMG signals from each contact of the thin-film structure (as well as the 64 surface electrodes in Experiment 2) were recorded with a multi-channel amplifier (EMG-USB2, OT Bioelettronica) with an amplification gain in the range 200–500. They were band-pass filtered (8th order Bessel filter, bandwidth 100–4400 Hz), before being sampled at 10 kHz, using a 12 bit A/D converter. The EMG signals were acquired in bipolar derivation for recordings from the ADM and GG muscles, and in unipolar derivation for recordings from the TA muscle with reference electrode at the ankle. A ground electrode was placed at the wrist (Experiment 1), ankle (Experiment 2), and shoulder (Experiment 3).

In the first two experiments, the subjects were asked to perform a series of isometric contractions (abduction of the little finger, Experiment 1, and ankle dorsi-flexion, Experiment 2). Specifically, the protocol of Experiment 1 included two 5 min contractions at 10% and 15% MVC, and Experiment 2 consisted of three 30 s contractions at 10, 20 and 30% MVC. In both experiments, a maximal force contraction was repeated at the end of the experiments. A period of rest of 2–10 min was provided between contractions, and increased under discretion of the subject, in order to prevent fatigue. Force was provided as feedback to the subject using a custom written software implemented in Matlab (The MathWorks, Inc., Natick, MA, USA). The subject was asked to maintain a red circle as close as possible to a trajectory that was shown on a screen in front of him. In Experiment 2, the submaximal contractions were repeated twice. In the first case, the surface EMG signals were recorded with the high-density grid of surface electrodes placed medially with respect to the thin-film structures. This placement was chosen to avoid the risk of accidentally removing the thin-film electrodes while overlying the grid. However, this resulted in few common MUs detected from both the surface and intramuscular EMG (see Results). To ascertain that the paucity of common MUs was not due to the relative positions of surface and intramuscular electrodes, the grid of surface electrodes was moved to overlap to the thin-film structures so that the central column was superimposed to the line connecting the two structures and the steady contractions at 10–30% MVC were repeated. In Experiment 3, the subject lay supine and breathed quietly through the nose and occasionally swallowed spontaneously.

Signal analysis

The experimental recordings involved different muscles and conditions with the purpose of assessing the signal quality, the type of information that could be extracted by

the recordings, the stability of the recording for changes in muscle force, and the range of potential applications. The signal quality was evaluated in terms of the baseline noise level, calculated as the average across channels of the root-mean-square of a 10 s segment of data recorded at rest, i.e. when no MUAPs appeared in the signals. The evaluation was repeated at the beginning and the end of the experimental session, separated by a few hours, in order to evaluate the signal quality degradation over time.

For the submaximal contractions recorded in Experiments 1 and 2, a 10 s interval where the force signal was approximately steady was identified and the EMG signals recorded in that interval were decomposed into the constituent MUAP trains using the interactive software EMGLAB (McGill *et al.* 2005). Each channel was decomposed independently of the others. In most cases, the same unit appeared in more than one channel (see Results: Signal decomposition, Figs 5, 6, 7 and 9). In these instances, the firing patterns of the same MU obtained in different channels were compared. Eventual discrepancies among different channels were resolved by visual inspection considering the overall information provided by all channels where that MU could be detected. This procedure was repeated for all channels until the residual, i.e. the signal that remains after the templates of the identified MUAPs have been subtracted from the interferential signal (McGill *et al.* 2005), was similar to the baseline noise in all channels. A set of unique MUs was identified and subject to further analysis, as detailed below.

MUs were characterized by the following parameters: mean firing rate, obtained as the average of the inverse of the inter-spike interval (ISI); the coefficient of variation (CoV) of the ISI, i.e. the ratio between its standard deviation and mean value; and the peak-to-peak amplitude of the template of each MU in the channel in which the amplitude was maximal. In Experiment 2, bipolar signals were derived offline by subtracting EMG from adjacent channels. Not all MUs were active for the entire interval of 10 s considered for calculating the physiological parameters. For those MUs which were recruited within the 10 s interval, the first second of signal after the initial discharge of that MU was excluded from the analysis in the calculation of the mean firing rate and the ISI CoV, because of the occurrence of doublets at recruitment (Denslow, 1948).

The template action potential of each MU for each of the 16 channels (15 in case of bipolar recordings) was calculated using spike-triggered averages. This allowed us to estimate the size of the MU territories. A MU is composed of fibres that are intermingled with the fibres belonging to other MUs. The MU territory is the region of the muscle occupied by the fibres innervated by a single MN (Bodine-Fowler *et al.* 1990). Therefore, the amplitude of the AP corresponding to each MU decreases with the distance of the detecting electrode site from the territory.

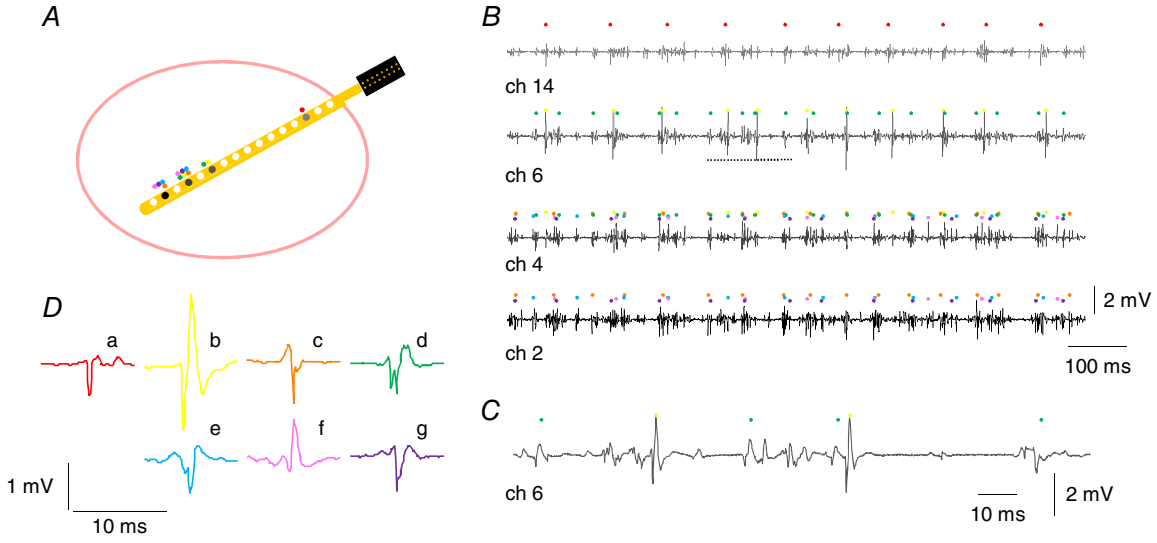

Figure 5. Electromyographic signal detection from a thin-film electrode structure implanted in the abductor digiti minimi muscle
A, cross-section of a simple muscle with the electrode array within. The array includes 16 detection sites (d_1–d_2–. . . –d_{16} from the tip towards the connector). *B*, four bipolar electromyographic signals obtained during an isometric contraction of the abductor digiti minimi muscle at 15% of the maximal force in Experiment 1. The potential v recorded at channel i is obtained as the difference of the potentials at two adjacent detection sites (with 1 mm inter-site distance): $v(ch_i) = v(d_i) - v(d_{i+1})$. Motor unit action potential trains are represented with colour-coded dots. Dots of the same colours are used in *A* to indicate the location of the motor units inside the muscle. *C*, a segment of the signal from channel 6 on a large time scale. *D*, template of the units represented in *B*, in the channel with the highest amplitude.

Consequently, the size of the territories (c) of the detected MUs could be estimated as $c = p.\sin(\alpha)$, where p is the distance between the first and the last detection sites where the average APs are above baseline noise and α is the insertion angle with respect to the muscle fibre direction. The value of p is therefore a multiple of the inter-site distance d (1 mm in our study).

One important characteristic of the electrode is the stability of the recorded signal for changes in muscle force. To assess this properly, we analysed the template AP of the same MUs identified in contractions with different forces. The peak of the normalized cross-correlation of the aligned 10 ms templates in the channel with the maximal amplitude was reported as a measure of the template similarity across contraction levels. If the shape similarity of APs across contractions at different forces was high, it was assumed that the electrode position with respect to the sources changed minimally with changes in muscle force.

Comparison with the MU activity detected from surface electrodes

Because recently it has been shown that multi-channel surface EMG decomposition also allows for the identification of the behaviour of several MUs, measurements were performed to show the differences in information extraction between multi-channel surface EMG and the proposed intramuscular electrode. In Experiment 2, we concurrently recorded intramuscular EMG signals with two thin-film structures and surface signals with a grid of 64 electrodes. Surface EMG signals were decomposed with the convolution kernel compensation (CKC) method, which was introduced by Holobar & Zazula (2007) and has been previously validated in muscles with different architectures (Holobar *et al.* 2009; Marateb *et al.* 2011*a*). The MUs extracted from the surface EMG were considered to be accurately identified if the CoV of the ISI was <30%, according to the criterion proposed in Holobar *et al.* (2014). For consistency, in the comparison between results obtained by the intramuscular and surface electrodes, the same criterion was applied for MUs identified from the thin-film electrode. The aim of the concurrent analysis of surface and intramuscular EMG signals was to assess whether the same information about the MU pool as that extracted with the thin-film intramuscular electrode could also be extracted with non-invasive methods, at least for superficial muscles.

To determine if common MUs were detected from the surface and intramuscular signals, we used the firing trains extracted from the surface EMG to trigger an average of the multi-channel intramuscular EMG. The averaging procedure would yield a template above the baseline noise in case of common MUs. The firing patterns of the MUs detected from both systems (surface and intramuscular) were compared by means of the accuracy index considering the decomposition results obtained from the intramuscular signals as a benchmark. The accuracy index (Acc) was defined as $\text{Acc} = (\text{TP} - \text{FP})/(\text{TP} + \text{FN})$, where TP (true positive) is the number of discharges identified by both types of EMG signals, FP (false positive) is the number of discharges not identified by the surface

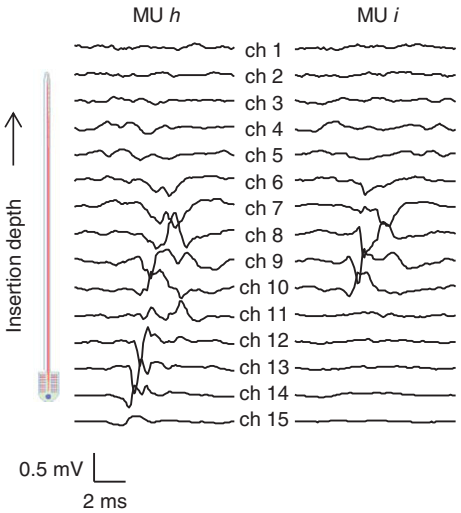

Figure 6. Motor unit territory
Average action potentials (templates) of two motor units (*h* and *i*) detected in Experiment 1 from the abductor digiti minimi muscle during an isometric contraction at 15% of the maximal force across 15 bipolar channels. The number of action potentials included in the average was 104 and 147 for the units *h* and *i*, respectively. Spike-triggered averaging resulted in amplitude similar to the background level for electrodes outside the motor unit territory.

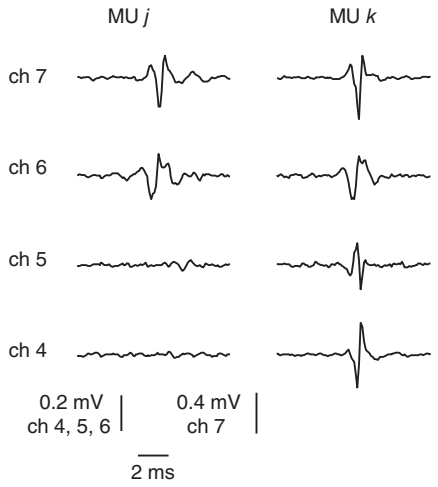

Figure 7. Multi-channel representation of motor units
Average action potentials (templates) of two motor units (*j* and *k*) detected from the abductor digiti minimi muscle during an isometric contraction at 15% of the maximal force in Experiment 1. The number of action potentials included in the average was 147 and 176 for the units *j* and *k*, respectively. Signals were high-passed filtered at 500 Hz prior to averaging. The templates of the two units are quite similar in channels 6 and 7 whereas only unit *k* appears in channels 4 and 5.

EMG signals, and FN (false negative) is the number of discharges identified by the surface EMG that did not match any discharge identified from the intramuscular signals (Marateb *et al.* 2011*b*).

Results

Signal decomposition

Figure 5*A* is a schematic drawing showing the cross-section of a simple muscle and the position of the thin-film electrode structure and sites of a transversely implanted device. For small muscles, e.g., the ADM (muscle diameter ~1.5 cm), the proposed electrode array would be able to sample from the entire muscle cross-section if inserted perpendicular to the skin. Figure 5*B* shows a 1 s interval of EMG data recorded from four channels of the electrode array in the ADM muscle during a 15% MVC contraction. Figure 5*C* is a 150 ms excerpt of channel 6. The dots on top of each EMG trace represent the highest amplitude MUAP trains in that channel. MUs are colour coded. The template with maximal amplitude in the considered channels is shown in Fig. 5*D*. The MUs that could be identified in each channel were more than those shown, for clarity, in the graphical representation.

In Fig. 5*A*, we represent the position of the MUs within the muscle with dots of the same colours as in Fig. 5*B* in proximity of the detection sites where those MUs were found. For example, MU *d* (dark green) was detected only by channels 4 and 6, because channels 2 and 14 were outside the territory of this MU. The size of the territory of a MU can be estimated from the spike-triggered averages across the 15 channels, as shown in Fig. 6 for two MUs identified from the same signal. In the two representative examples shown in Fig. 6, a territory cord of about 4 mm can be inferred for MU *h* considering the inter-site distance (1 mm), the insertion angle (30 deg), and that the templates span about eight channels. For MU *i*, four channels resulted in a territory of about 2 mm.

The fact that the same MU usually appeared in more than one channel was exploited to obtain an accurate decomposition of the intramuscular EMG into the constituent MUAP trains. In each EMG channel, those MUs with closest territory to the electrode site had higher amplitude APs and the corresponding firing patterns could be identified with high confidence. The identification of the firing patterns of MUs with low amplitude APs would have been more challenging if only one channel was available. However, these MUs could be usually identified better in other channels. In general, although the decomposition software can handle multi-channel signals, signal decomposition was applied to each EMG channel independently. Firing patterns with time-locked discharges were identified as belonging to the same MU detected on different channels; eventual mismatches among time-locked spike trains were resolved by visually inspecting the multi-channel representation. The information provided by multiple channels was also beneficial because two MUs may have similar templates in one channel and different templates in another channel, as shown with a representative example in Fig. 7.

Detected motor unit populations

Figure 8 shows the MUAP trains identified by decomposing the EMG signals recorded from the ADM during

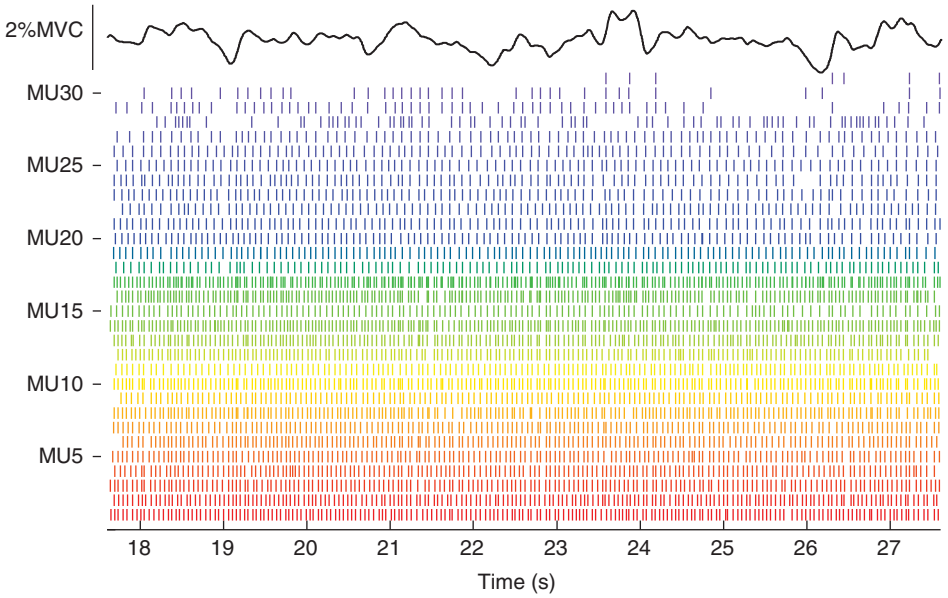

Figure 8. Representative firing pattern of motor units from abductor digiti minimi
Firing patterns of 31 motor units detected in Experiment 1 during an isometric contraction of the abductor digiti minimi muscle using the thin-film electrode. Force exerted during the contraction is also shown, 15% of maximum.

Table 1. Number of motor units detected in the signals recorded from the tibialis anterior muscle with the thin-film electrodes in Experiment 2

		Contraction level (% MVC)					
		10	20	30	10–20–30	10–20	20–30
Electrode	Proximal	38	45	44	23	11	10
	Distal	40 (25)	46 (34)	50 (34)	24	9	13

The number in parentheses indicates the common motor units detected from electrode structures in the proximal and distal locations. The number of motor units common to the three force levels is indicated in the column 10–20–30, whereas the columns 10–20 and 20–30 report the number of extra units commonly to the two lower and higher contraction levels, respectively.

a sustained contraction at 15% MVC. Approximately 30 MUs were identified, which presumably corresponded to about one-third of the population of MUs active at that force intensity considering that the ADM muscle has approximately 380 MUs (Santo Neto *et al.* 1985) and it is likely to complete its recruitment at about 50% MVC, as with most small hand muscles (De Luca *et al.* 1982). This number would be further increased in the case of insertion of the electrode structure perpendicular to the muscle fibre direction, which maximizes the portion of the muscle cross-section from which the electrode can sample. The insertion angle adopted in Experiment 1 aimed to have the full electrode array within the muscle (the ADM diameter was measured by ultrasound at less than 15 mm).

In Experiment 2, in which the electrode was inserted perpendicular to the skin, up to 46 and 50 MUs were detected at 20 and 30% MVC contraction levels, respectively, with only one electrode (Table 1). Representative recordings for this experiment are shown in Fig. 9. An interval of 1 s is shown for the 16 recordings, with coloured symbols indicating the identified MU discharge timings. From this raw data, it is also possible to observe the high signal-to-noise ratio of all the recordings. Twenty-seven MUs are shown in Fig. 9, which corresponded to only a subset of all 39 identified MUs in this recording (a reduced number of MUs is shown for clarity in the figure).

Physiological parameters of the MUs extracted from a sample of contractions included in the experimental protocols 1 and 2 are shown in Table 2. The firing rate and CoV for the MUs in the ADM were similar to those reported previously with classic recording systems (Negro *et al.* 2009). For the TA muscle, the firing rate increased with the force intensity (e.g. Connelly *et al.* 1999) and the ISI CoV was higher at 10 than 20% MVC because some MUs detected at the lowest contraction level were close to the recruitment threshold and had a more irregular firing pattern at 10% MVC. A further increase of the force level from 20 to 30% MVC determined an increase in the CoV of ISI as well (Jesunathadas *et al.* 2012).

Signal stability over time

No degradation of the signal quality was observed through the course of the experiments. At the end of the experimental session, when the thin-film electrode was in the muscle for approximately 2 h, the average noise RMS ($\pm$ standard deviation) across channels was 19 ± 6 μV in Experiment 1 and 12 ± 6 μV in Experiment 2.

In Experiment 1, 12 out of the 14 MUs detected during the sustained contraction at 10% MVC were also detected during the contraction at 15% MVC. The average cross-correlation across the templates of those 12 MUs was 0.89 ± 0.04. The systematic analysis of template similarities across contraction forces for the TA (Experiment 2) is reported in Table 3. Figure 10 shows representative examples of MUs identified at 10% MVC and tracked at 20 and 30% MVC (average cross-correlation >0.9 in this example). These results indicate that the change in muscle force minimally influenced the electrode position with respect to the active muscle fibres and therefore indicate the stability of the thin-film structure in the muscle.

Comparison with the information extracted from the surface EMG decomposition

Surface EMG signals were recorded along with intramuscular EMG in Experiment 2. In the same intervals considered for the analysis of the intramuscular signals (Table 1), the surface EMG decomposition yielded 34, 40 and 36 spike trains (CoV $\leq$ 30) at 10, 20 and 30% MVC, respectively. Their average firing rate is reported in Table 2 along with the CoV for ISI. Firing rates are similar to those found for the MUs extracted from intramuscular signals whereas both the mean and standard deviation of the CoV values were higher than those estimated from the intramuscular EMG. Only one MU in common between surface and intramuscular signals was found for the 20% MVC contraction level. The common MU was detected by sites 11–16 of the proximal structure and 10–16 of the distal structure, which are the most

superficial sites. Two FPs and two FNs were present in the AP train identified by the CKC algorithm for that MU, which resulted in an accuracy of decomposition of 97%.

When the grid of surface electrodes overlapped the insertion point of the thin-film electrodes, the decomposition of the surface EMG provided 19, 14 and 15 MUs at the three force intensities. Of these units, only 2, 1 and 1 resulted exceeding the baseline noise levels in the most superficial electrode sites of the thin-film structures after spike-triggered averaging. The consistent finding of very few MUs detected commonly between surface and the thin-film structures indicates that the surface EMG samples from an extremely superficial layer of the muscle. This is in agreement with simulations that showed that the decomposition of surface EMG provides MUs at a depth of up to few millimetres (see e.g. Fig. 3 in Holobar *et al.* 2009). Therefore, the information extracted by the proposed thin-film structure is not redundant and cannot be obtained with other techniques.

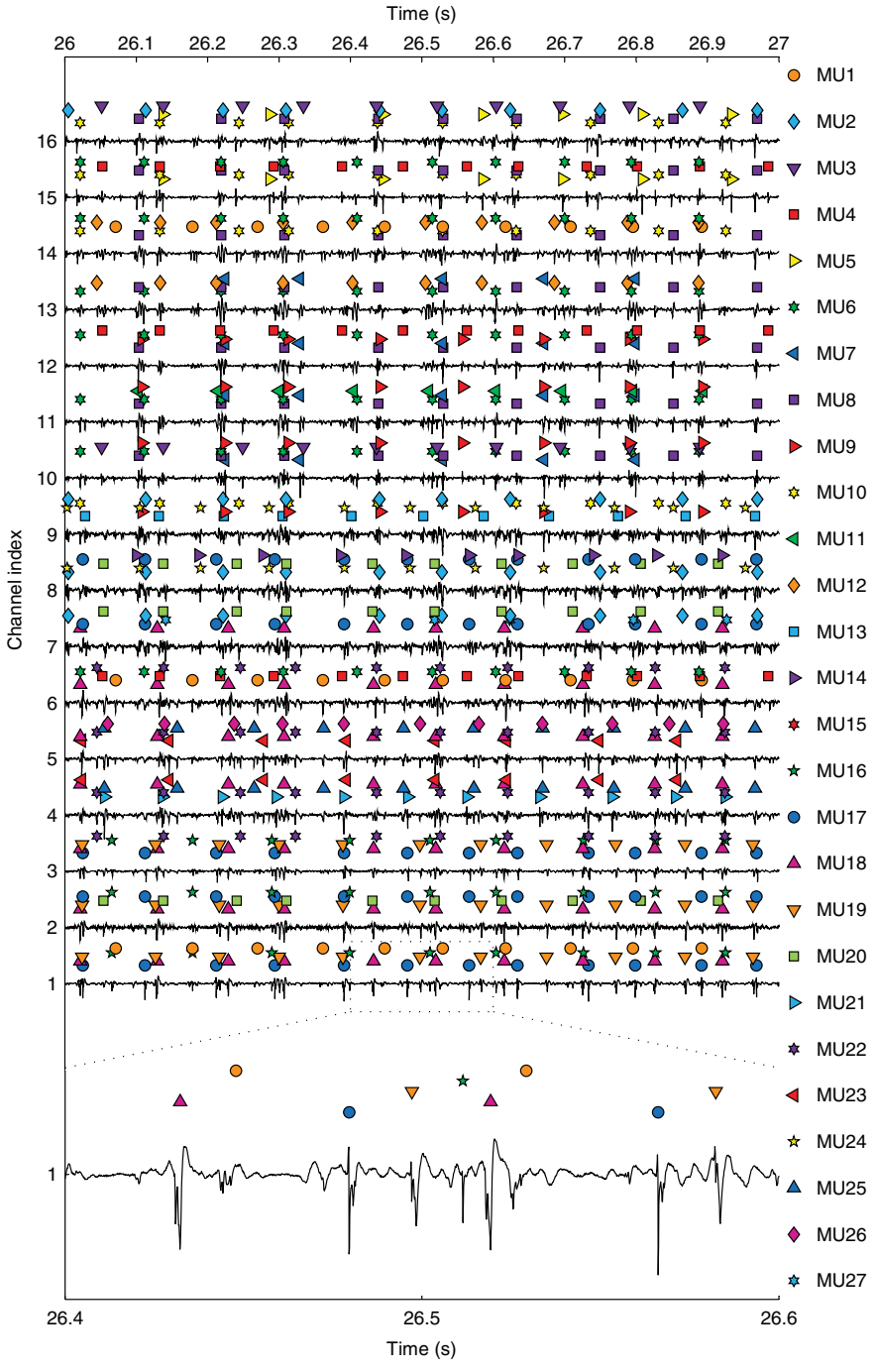

Figure 9. Representative recordings from tibialis anterior
A 1 s segment to show EMG signals acquired from the 16 detection sites on the thin-film electrode inserted in the distal position in the tibialis anterior in Experiment 2. Electromyographic signals are normalized to the maximal peak-to-peak amplitude across the entire contraction relative to each channel. The discharges of the 5 motor units with the highest average action potential peak-to-peak amplitude are shown above each electromyographic trace. Different motor units are represented with different coloured symbols (see legend on the right). The contraction force was 10% of the maximal force. A 200 ms segment of the signal from channel 1 is shown at the lowest part of the figure.

Table 2. Signal characteristics for intramuscular and surface recordings made in Experiments 1 and 2

Experiment ID	Contraction level (%MVC)	Electrode ID	Number of MUs (in 10 s intervals)	Firing rate (mean ± SD) (Hz)	Coefficient of variation of the inter-spike interval (%)	Peak-to-peak unipolar amplitude (mean ± SD) (mV)	Peak-to-peak bipolar amplitude (mean ± SD) (mV)
1	10		23	15.6 ± 4.5	20.6 ± 7.5		1.14 ± 0.79
	15		31	15.5 ± 4.8	22.3 ± 8.3		1.15 ± 0.68
2	10	P	34 (−4)	9.9 ± 1.3	13.2 ± 3.2	0.87 ± 0.45	0.77 ± 0.47
		D	37 (−3)	9.9 ± 1.3	13.6 ± 4.6	0.79 ± 0.43	0.72 ± 0.46
		S	34	9.2 ± 1.1	17.1 ± 4.7		
	20	P	45	13.2 ± 1.2	10.7 ± 2.0	0.92 ± 0.49	0.77 ± 0.46
		D	46	13.1 ± 1.1	10.3 ± 1.6	0.88 ± 0.43	0.77 ± 0.49
		S	40	12.1 ± 1.2	14.4 ± 4.7		
	30	P	44	13.8 ± 1.8	12.5 ± 2.0	1.12 ± 0.58	0.94 ± 0.53
		D	50	14.0 ± 1.6	12.3 ± 1.9	0.96 ± 0.38	0.77 ± 0.40
		S	36	12.8 ± 1.3	15.3 ± 4.5		

SD, standard deviation; P, proximal; D, distal; S, surface. Amplitude refers to the mean ± SD of the amplitude across all the motor units (MUs) indicated in the column 'Number of MUs'. For each MU, the maximal amplitude across the channels was considered. For Experiment 1, doublets were eliminated before the calculation of the coefficient of variation of the inter-spike interval. Four and three MUs identified from the signals detected with the proximal and distal thin-film electrodes, respectively, were eliminated from the analysis according to the selected criterion for the determination of accurately decomposed MUs (CoV > 30).

Table 3. Template similarity across contractions levels recorded in Experiment 2

		Contraction levels (% MVC)		
		10–20	10–30	20–30
Electrode	Proximal	0.95 ± 0.06 (34)	0.93 ± 0.05 (23)	0.96 ± 0.02 (33)
	Distal	0.95 ± 0.05 (33)	0.95 ± 0.03 (21)	0.95 ± 0.05 (37)

Mean ± standard deviation of the peak of the normalized cross-correlation of the templates of the motor units common to contractions at force intensities indicated in the header. The template had a time support of 10 ms and was calculated from the channel where the action potential had maximal amplitude. The number of common motor units between contraction levels is indicated in parentheses.

Recording from a deep muscle

To further demonstrate the utility of the new thin-film electrode to alternative techniques, such as multi-channel surface EMG decomposition, in Experiment 3 the thin-film electrode was used to record activity from the GG muscle of a subject who was breathing quietly. Figure 11 shows two EMG signals (panel *A*) recorded during two quiet breaths and the discharge trains of the five MUs extracted from those two channels (panel *B*). The mean firing rate was 19.2 ± 4.0 Hz across the five MUs, quite high as previously reported (e.g. Saboisky *et al.* 2006). The two channels shown in Fig. 11*A* are the only channels in which EMG signals were detected during quiet breathing. However, this absence of activity was not due to malfunctioning of the thin-film structure. Indeed, when the subject swallowed, EMG appeared in all channels (Fig. 11*C*). In this example, the recorded EMG activity provides data not only on the discharge behaviour of active MUs but also on their location inside the muscle.

Discussion

We report the design, fabrication and testing in three human muscles of a novel multi-channel thin-film electrode for intramuscular EMG recordings.

Detection of large population of motor units from superficial and deep muscles

The proposed electrode allowed concurrent recordings of a relatively large proportion of the MUs active during contractions at different forces. Most of the current knowledge of MU physiology is based on the interpretation of sets of serially recorded single MU activity collected from different trials and subjects (e.g. Bigland-Ritchie *et al.* 1983; Butler *et al.* 1999; Saboisky *et al.* 2006, 2007) or by multiple electrode insertions within a muscle (e.g. Vieira *et al.* 2011; Héroux *et al.* 2014). The proposed structure provides the possibility of concurrently sampling intramuscular EMG activity from

the entire muscle cross-section. About 30 MUs could be identified at relatively low force levels (15% MVC) from the ADM muscle. Up to 50 were detected from the TA using only one thin-film electrode structure (Table 1). One of the advantages of having simultaneous recordings of many MUs is the possibility of increasing the bandwidth of MU correlation measures in the frequency domain, e.g. coherence (Negro & Farina 2012). In the case of the GG muscle, few MUs were detected (Fig. 11*B*), which is likely to be because the quiet breathing involves less GG activation compared with other tasks such as swallowing (Fig. 11*C*).

Recently, it has been demonstrated that MU discharge times can also be identified from multi-channel surface EMG (e.g. Holobar *et al.* 2009). However, surface EMG decomposition only allows identification of MUs with large surface APs (which are limited to the superficial portion of the muscle), whereas intramuscular electrodes allow recording also from deep muscle portions. When we concurrently used the thin-film structures and a grid of surface electrodes to record EMG from the TA muscle, we accessed two almost separate populations because the intramuscular electrodes were deeper than the detection area of the surface electrodes in Experiment 2. The few MUs commonly detected were limited to the most superficial electrode sites of the thin-film electrodes. Conversely, the new electrode samples at different depths and thus provides a more representative distribution of active MUs in a muscle.

The new intramuscular electrode is even more useful for muscles which are difficult to assess both with classic intramuscular and with surface electrodes. As an example, we have presented representative recordings from the GG muscle. This muscle has been the object of intensive recent investigation because of its role in maintaining patency of the human upper airway (Saboisky *et al.* 2006; Wilkinson *et al.* 2010). There is currently no technology for recording high-density high-quality surface EMG accessing the GG from the oral cavity. MU activity cannot even be retrieved from decomposition of surface EMG signals detected at the bottom of the chin as the geniohyoid muscle is interposed between the GG and the skin reducing the size of the GG APs obtainable at the skin surface. Spatial sampling of the muscle with needles has been performed moving the needle in multiple sites (with up to three needle insertions) (Saboisky *et al.* 2006, 2007). However, this procedure cannot provide exact information about the location where muscle activity was sampled and does not allow the concurrent analysis of the behaviour of MUs in different muscle locations.

The proposed polyimide-based structure comprises an array of detection sites arranged in a consistent geometry which can only be obtained by the use of microfabrication technologies. This opens the possibility of sampling muscle activity in specific positions and to relate the muscle electrical activity to spatial information. Moreover, it allows obtention of reproducible measures across subjects. Additionally, due to its polyimide substrate, the microfabricated electrode is flexible and can hardly be felt once the needle used for insertion has been removed. Therefore, it allows strong contractions without discomfort (up to maximal force) and can be used for long-lasting recording, e.g. during sleep, when the use of needles would be uncomfortable and the use of surface electrodes would be hindered by the degradation of the skin–electrode contact quality over time. In the experiments reported here, the noise level was similar through the duration of the recording session. Moreover, the similarity in MU templates across different

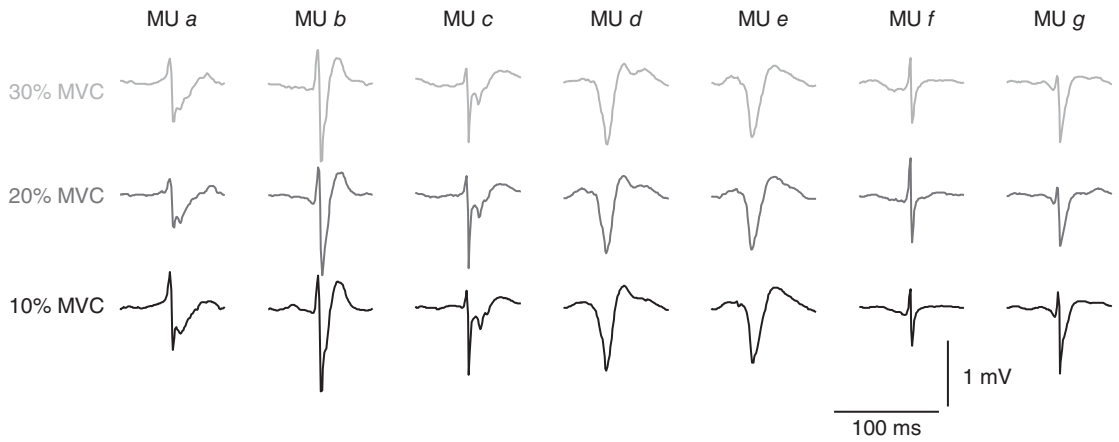

Figure 10. Template similarity across contractions levels
Average action potentials (templates) of 7 representative common motor units detected from the tibialis anterior muscle during isometric contractions at 10% (black), 20% (dark grey) and 30% MVC (light grey) in Experiment 2. The templates are highly similar across the three contraction intensities, which indicates that the electromyographic signals were stable over time.

contractions (Table 3 and Fig. 10) suggests that the relative movement between source and detecting electrode was minimal.

Motor unit territory

One application of the multi-channel thin-film electrode is the study of the MU territory, i.e. the portion of a muscle where the majority of the fibres of a MU are located. The gold standard for determination of the territory size is the scanning EMG procedure (Stålberg & Antoni, 1980) that requires the use of two indwelling electrodes, a single fibre EMG electrode to trigger the activity from one MU and a scanning needle electrode that detects activity synchronous with that from the triggering electrode. The triggering electrode has to be moved in a number of positions corresponding to the number of investigated MUs. For each of those positions the scanning electrode is moved along a corridor until no APs corresponding to the triggering MU are detected. The proposed multi-channel structure allows the determination of the size of the territory of several MUs at a time.

The spatial resolution in the estimation of MU territories depends on the inter-site distance. A relevant characteristic of the intramuscular electrode described here is that the number of electrode sites and inter-site distance can be tailored to specific applications. In the representative recordings we presented, the inter-site distance was 1 mm, so that the 16 electrode site array could sample from a 15 mm long portion of the muscle. This length approximately corresponds to the ADM diameter and the GG width (Saboisky *et al.* 2006). However, the inter-site distance and the number of electrode sites can be extended depending on the cross-section of the muscle targeted for investigation. The inter-site distance can also be decreased to increase spatial resolution.

Decomposition accuracy

Another application of the presented electrode is to improve the accuracy of MU decomposition by multi-channel MU representation. Indeed, the simultaneous representation of the same MU activity at different

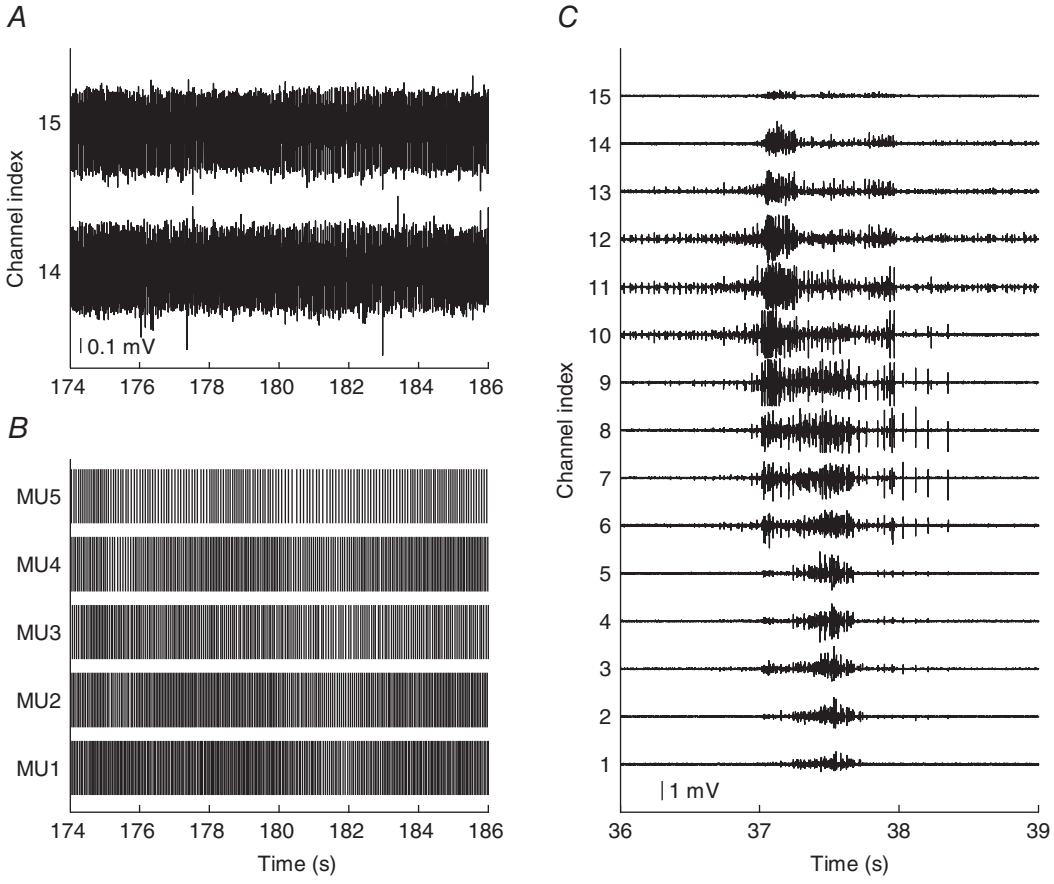

Figure 11. Representative signals from genioglossus
A, two channels of electromyographic signals recorded from the genioglossus muscle during quiet breathing through the nose. *B*, motor unit action potential trains contributing to the composite signals in *A*. *C*, electromyographic signals recorded from 15 bipolar channels during a spontaneous swallow. The signals shown in the left and right panels belong to two blocks of data (~3.5 min) recorded approximately 2.5 h apart.

electrode sites can be exploited to eliminate ambiguity in the identification of individual MUAPs (Florestal *et al.* 2009). For example, waveforms produced by the superimposition of several MUAPs may be more easily identified in one channel than in others. Moreover, it may happen that a MU that appears in a channel where there is a superimposition difficult to resolve may be absent in another channel or that two MUs that have similar templates in a channel have different templates in another one (Fig. 7). When a multi-channel EMG signal is available, a valuable indication of a correct decomposition is provided when all firing occurrences of a certain MU are locked-in to the occurrences in all channels where the same unit appears and the residual signal after template matching is similar to the baseline noise level in all channels, as occurred in our analysis. Therefore, the accuracy of decomposition with the new electrode is likely to be superior to that with both single-channel intramuscular EMG and multi-channel surface signals. The fact that the CoV of the ISI of the MU population extracted from surface signals was higher on average for the surface decomposition (Table 2) may indicate that the firing patterns obtained from the surface EMG were less regular, and thus that surface EMG decomposition provided less accurate results.

Conclusions

We have presented the design, fabrication and testing of a new multi-channel thin-film electrode for detection of the output of human MNs *in vivo* from EMG signals. Tests revealed that the electrode allows simultaneous recordings of a large proportion of the active MUs providing a viable technology to investigate the neural drive to muscles with high accuracy. The structure represents a novel technology for electrophysiological investigations in muscles and its design characteristics (e.g. number of electrodes, inter-site distance) can be easily tailored to the muscle under investigation and the required analysis.

References

Adrian ED & Bronk DW (1929). The discharge of impulses in motor nerve fibres. Part II. The frequency of discharge in reflex and voluntary contractions. *J Physiol* **67**, 119–151.

Basmajian J & Stecko G (1962). A new bipolar electrode for electromyography. *J Appl Physiol* **17**, 849.

Bigland-Ritchie B, Johansson R, Lippold OC, Smith S & Woods JJ (1983). Changes in motoneurone firing rates during sustained maximal voluntary contractions. *J Physiol* **340**, 335–346.

Bodine-Fowler S, Garfinkel A, Roy RR & Edgerton VR (1990). Spatial distribution of muscle fibers within the territory of a motor unit. *Muscle and Nerve* **13**, 1133–1145.

Butler JE, McKenzie DK & Gandevia SC (1999). Discharge properties and recruitment of human diaphragmatic motor units during voluntary inspiratory tasks. *J Physiol* **518**, 907–920.

Connelly DM, Rice CL, Roos MR & Vandervoort AA (1999). Motor unit firing rates and contractile properties in tibialis anterior of young and old men. *J Appl Physiol* **87**, 843–852.

De Luca C & Forrest WJ (1972). An electrode for recording single motor unit activity during strong muscle contractions. *IEEE Rev Biomed Eng* **19**, 367–372.

De Luca CJ, LeFever RS, McCue MP & Xenakis AP (1982). Behaviour of human motor units in different muscles during linearly varying contractions. *J Physiol* **329**, 113–128.

Denslow JS (1948). Double discharges in human motor units. *J Neurophysiol* **11**, 209–215.

Farina D & Enoka RM (2011). Surface EMG decomposition requires an appropriate validation. *J Neurophysiol* **105**, 981–982; author reply 983–984.

Farina D, Holobar A, Merletti R & Enoka RM (2010). Decoding the neural drive to muscles from the surface electromyogram. *Clin Neurophysiol* **121**, 1616–1623.

Farina D, Merletti R, Indino B, Nazzaro M & Pozzo M (2002). Surface EMG crosstalk between knee extensor muscles: experimental and model results. *Muscle Nerve* **26**, 681–695.

Farina D & Negro F (2012). Accessing the neural drive to muscle and translation to neurorehabilitation technologies. *IEEE Rev Biomed Eng* **5**, 3–14.

Farina D, Yoshida K, Stieglitz T & Koch KP (2008). Multichannel thin-film electrode for intramuscular electromyographic recordings. *J Appl Physiol* **104**, 821–827.

Florestal JR, Mathieu PA & McGill KC (2009). Automatic decomposition of multichannel intramuscular EMG signals. *J Electromyogr Kinesiol* **19**, 1–9.

Héroux ME, Dakin CJ, Luu BL, Inglis JT & Blouin J-S (2014). Absence of lateral gastrocnemius activity and differential motor unit behavior in soleus and medial gastrocnemius during standing balance. *J Appl Physiol* **116**, 140–148.

Holobar A, Farina D, Gazzoni M, Merletti R & Zazula D (2009). Estimating motor unit discharge patterns from high-density surface electromyogram. *Clin Neurophysiol* **120**, 551–562.

Holobar A, Minetto MA & Farina D (2014). Accurate identification of motor unit discharge patterns from high-density surface EMG and validation with a novel signal-based performance metric. *J Neural Eng* **11**, 016008.

Holobar A & Zazula D (2007). Multichannel blind source separation using convolution kernel compensation. *IEEE Trans Signal Process* **55**, 4487–4496.

Jesunathadas M, Klass M, Duchateau J & Enoka RM (2012). Discharge properties of motor units during steady isometric contractions performed with the dorsiflexor muscles. *J Appl Physiol* **112**, 1897–1905.

Keenan KG, Farina D, Maluf KS, Merletti R & Enoka RM (2005). Influence of amplitude cancellation on the simulated surface electromyogram. *J Appl Physiol* **98**, 120–131.

Hoffmann KP & Koch KP (2005). Final report on design consideration of tLIFE2. tech. rep. IBMT 2005.

Liddell EGT & Sherrington CS (1925). Recruitment and some other Features of Reflex Inhibition. *Proc R Soc L B Biol Sci* **97**, 488–518.

Marateb HR, McGill KC, Holobar A, Lateva ZC, Mansourian M & Merletti R (2011*a*). Accuracy assessment of CKC high-density surface EMG decomposition in biceps femoris muscle. *J Neural Eng* **8**, 066002.

Marateb HR, Muceli S, McGill KC, Merletti R & Farina D (2011*b*). Robust decomposition of single-channel intramuscular EMG signals at low force levels. *J Neural Eng* **8**, 066015.

McGill KC, Lateva ZC & Marateb HR (2005). EMGLAB: An interactive EMG decomposition program. *J Neurosci Methods* **149**, 121–133.

Merletti R & Farina D (2009). Analysis of intramuscular electromyogram signals. *Philos Trans A Math Phys Eng Sci* **367**, 357–368.

Mesin L, Merletti R & Rainoldi A (2009). Surface EMG: The issue of electrode location. *J Electromyogr Kinesiol* **19**, 719–726.

Meyer JU, Stieglitz T, Scholz O, Haberer W & Beutel H (2001). High density interconnects and flexible hybrid assemblies for active biomedical implants. *IEEE Trans Adv Packag* **24**, 366–374.

Negro F & Farina D (2012). Factors influencing the estimates of correlation between motor unit activities in humans. *PLoS One* **7**, e44894.

Negro F, Holobar A & Farina D (2009). Fluctuations in isometric muscle force can be described by one linear projection of low-frequency components of motor unit discharge rates. *J Physiol* **587**, 5925–5938.

Poppendieck W, Hoffmann K-P, Rocon E, Pons JL, Muceli S, Dideriksen J & Farina D (2014*a*). Multi-channel EMG recording and muscle stimulation electrodes for diagnosis and treatment of tremor. In *2014 IEEE 19th International Functional Electrical Stimulation Society Annual Conference (IFESS)*, pp. 14–17.

Poppendieck W, Muceli S, Welsch C, Krob MO, Sossalla A, Yoshida K, Farina D & Hoffmann KP (2013). Development of multi-channel intramuscular EMG recording electrodes. *Biomed Eng (NY)*; DOI: 10.1515/bmt-2013-4.

Poppendieck W, Sossalla A, Krob MO, Welsch C, Nguyen TAK, Gong W, DiGiovanna J, Micera S, Merfeld DM & Hoffmann KP (2014*b*). Development, manufacturing and application of double-sided flexible implantable microelectrodes. *Biomed Microdevices* **16**, 837–850.

Rossini PM, Micera S, Benvenuto A, Carpaneto J, Cavallo G, Citi L, Cipriani C, Denaro L, Denaro V, Di Pino G, Ferreri F, Guglielmelli E, Hoffmann KP, Raspopovic S, Rigosa J, Rossini L, Tombini M & Dario P (2010). Double nerve intraneural interface implant on a human amputee for robotic hand control. *Clin Neurophysiol* **121**, 777–783.

Saboisky JP, Butler JE, Fogel RB, Taylor JL, Trinder JA, White DP & Gandevia SC (2006). Tonic and phasic respiratory drives to human genioglossus motoneurons during breathing. *J Neurophysiol* **95**, 2213–2221.

Saboisky JP, Butler JE, McKenzie DK, Gorman RB, Trinder JA, White DP & Gandevia SC (2007). Neural drive to human genioglossus in obstructive sleep apnoea. *J Physiol* **585**, 135–146.

Santo Neto H, de Carvalho V & Penteado C (1985). Motor units of the human abductor digiti minimi. *Arch Ital Anat Embriol* **90**, 47–51.

Stålberg E & Antoni L (1980). Electrophysiological cross section of the motor unit. *J Neurol Neurosurg Psychiatry* **43**, 469–474.

Stieglitz T, Beutel H, Schuettler M & Meyer J-U (2000). Micromachined, polyimide-based devices for flexible neural interfaces. *Biomed Microdevices* **2**, 283–294.

Vieira TMM, Loram ID, Muceli S, Merletti R & Farina D (2011). Postural activation of the human medial gastrocnemius muscle: are the muscle units spatially localised? *J Physiol* **589**, 431–443.

Wilkinson V, Malhotra A, Nicholas CL, Worsnop C, Jordan AS, Butler JE, Saboisky JP, Gandevia SC, White DP & Trinder J (2010). Discharge patterns of human genioglossus motor units during arousal from sleep. *Sleep* **33**, 379–387.

Yoshida K & Stein RB (1999). Characterization of signals and noise rejection with bipolar longitudinal intrafascicular electrodes. *IEEE Trans Biomed Eng* **46**, 226–234.

Additional information

Competing interests

None of the authors have any conflicts of interests.

Author contributions

S.M., W.P., K.Y., K.H. and D.F. developed the multi-channel intramuscular thin-film electrode. S.M., F.N., J.B., S.G. and D.F. designed and performed the experiments. S.M. analysed the data. S.M. and W.P. prepared figures. S.M. and D.F. drafted the manuscript. All authors revised and approved the final version. Experiments were conducted at the Department of Neurorehabilitation Engineering, Georg-August University, Göttingen, Germany and Neuroscience Research Australia (NeuRA), Sydney, Australia.

Funding

This work was supported by the European Research Council (ERC) via the ERC Advanced Grant DEMOVE (No. 267888).

Acknowledgements

The authors sincerely thank Drs Julian P. Saboisky, Martin E. Héroux and Billy L. Luu for collaboration on the experimental recording procedures. J.B. and S.G. are supported by the National Health and Medical Research Council.